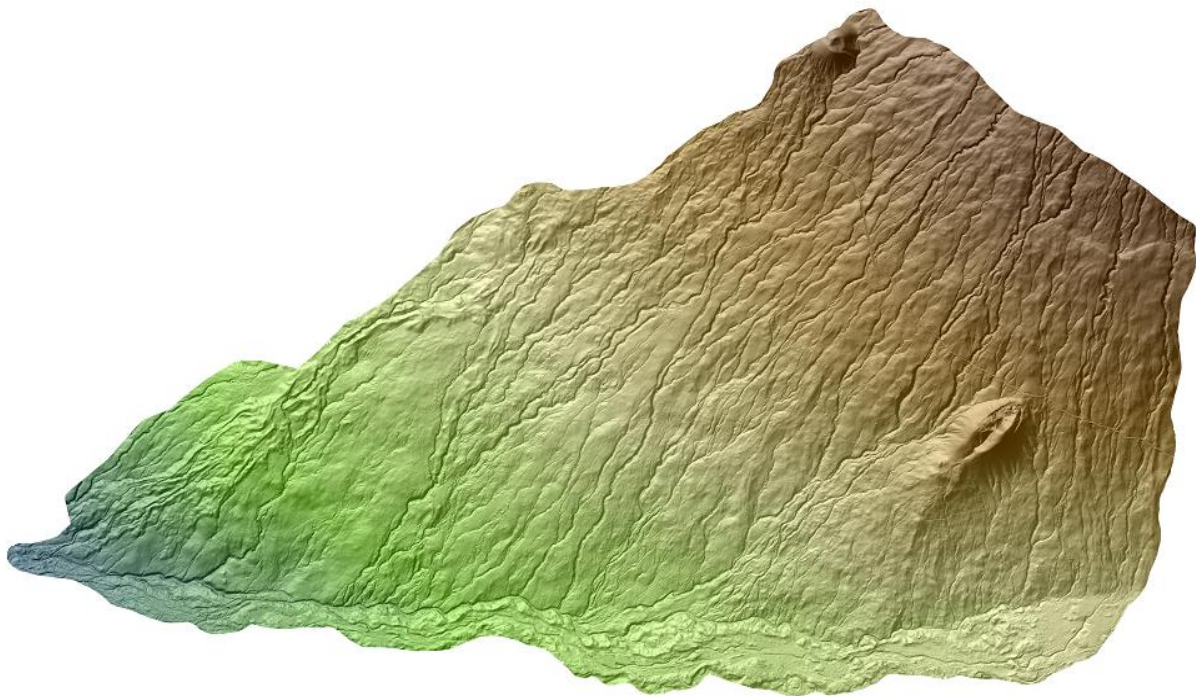


Office for Coastal Management - National Ocean Service - National Oceanic and Atmospheric Administration - U.S. Department of Commerce

# LiDAR for Pelekane Watershed

South Kohala District, Hawaii Island

Project Report – October 2015



Prepared by:

Tetra Tech Geomatic Technologies Group

3746 Mount Diablo Blvd Suite 300

Lafayette, CA 94549



## Table of Contents

Airborne LiDAR Acquisition.....	3
Tiling Scheme .....	5
LiDAR Quality Assessment .....	7
Data format.....	7
Trajectory.....	7
Coverage and swath-to-swath reproducibility .....	11
Absolute accuracy.....	16
Global analysis .....	18
Analysis by soil cover category .....	21
Point Density.....	22
Final product overview .....	26
Projection/Datum and Units.....	27
Deliverables.....	27

## Table of Figures

Figure 1: Pelekane watershed, LiDAR mapping extent.....	3
Figure 2: Aircraft trajectories overlaid with the project boundary.....	4
Figure 3: Processing tiling scheme AOI and AOI-buffer overlaid with the LiDAR data (intensity view). .....	5
Figure 4: Delivery tiling scheme and AOI-buffer for the Pelekane watershed. ....	6
Figure 5: Raw LiDAR files format and statistics.....	8
Figure 6: Trajectory accuracy for the August 25, 2015 acquisition. ....	9
Figure 7: Trajectory accuracy for the August 26, 2015 acquisition. ....	10
Figure 8: Swath overlap differences in meters for a 1m-cell grid, using single returns only. ....	12
Figure 9: Two zooms over the swath-to-swath image (in meters). ....	13
Figure 10: Seamlines between overlapping flightlines. ....	14
Figure 11: Distribution of inter-swath departure for 8229 seed points. ....	15
Figure 12: Spatial distribution of the 37 GCP over the project area.....	17
Figure 13: Residuals distribution computed on 35 GCP. ....	18
Figure 14: Distribution of the residuals computed with 35 GCP after the LiDAR global shift. ....	19
Figure 15: Residuals values overlaid with a map of the project area. ....	20
Figure 16: Comparison between VVA and NVA Ground Control Points.....	21
Figure 17: First return point density computed for each LiDAR tile. ....	22
Figure 18: Representative area (1 sq. km) for point density and spatial distribution assessment. ....	23
Figure 19: Point density grid, 50 cm cell size. ....	24
Figure 20: Digital Elevation Model – 1 meter grid combined with the corresponding hillshade and the AOIs.....	26

## Airborne LiDAR Acquisition

Tetra Tech was contracted by the National Oceanic and Atmospheric Administration (NOAA) to provide airborne LiDAR data for an area of about 15 square miles in the south Kohala district on the Hawaii Island (Big Island). The LiDAR data will support local hydrologists and watershed managers in their decision-making processes for the Pelekane watershed. The project area is presented on the figure below. This report presents the details of the acquisition as well as the quality checks that have been performed on the datasets.

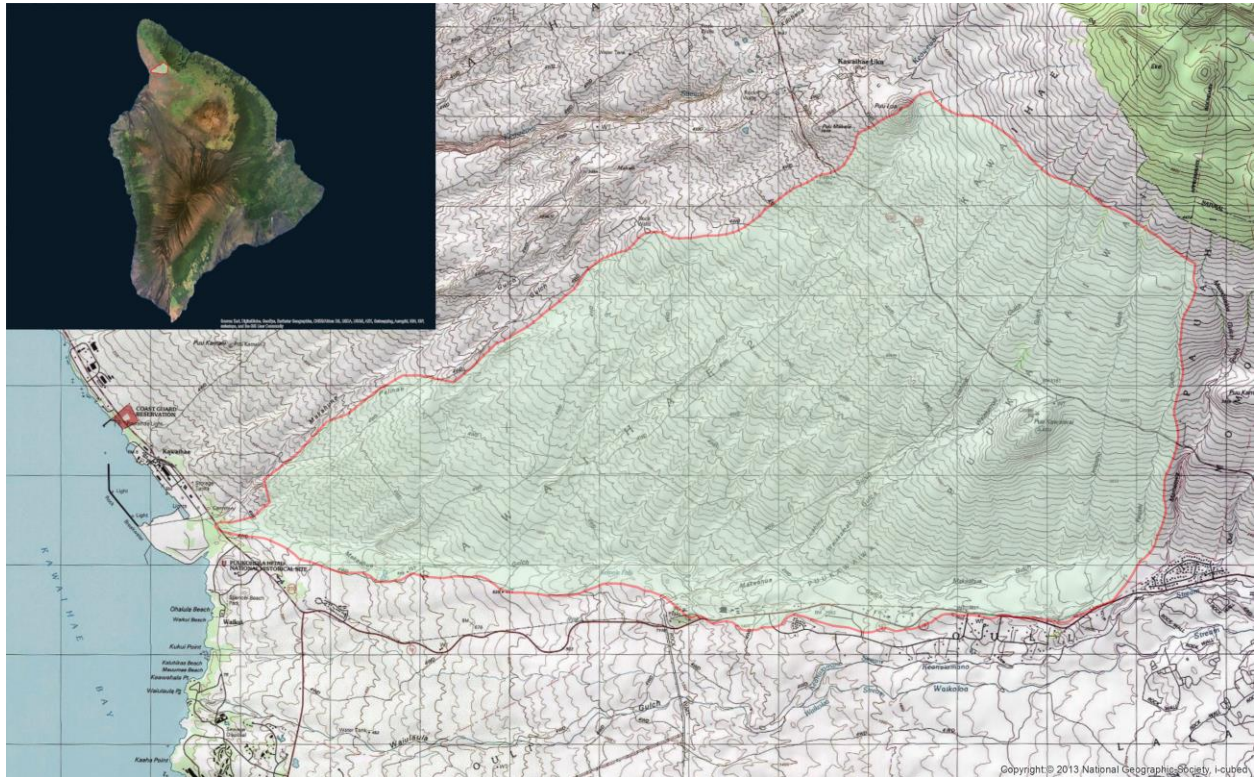


**Figure 1: Pelekane watershed, LiDAR mapping extent.**

The LiDAR acquisition took place on August 25, 2015 (in blue on the figure below) and on August 26, 2015 (in orange on the figure below). The LiDAR data has been collected using an Optech Orion M300 system. During both flights, the airborne trajectory has been monitored with kinematic AGPS combined with IMU observations collected at 200 Hz. The following picture shows the aircraft trajectories overlaid over the project area.

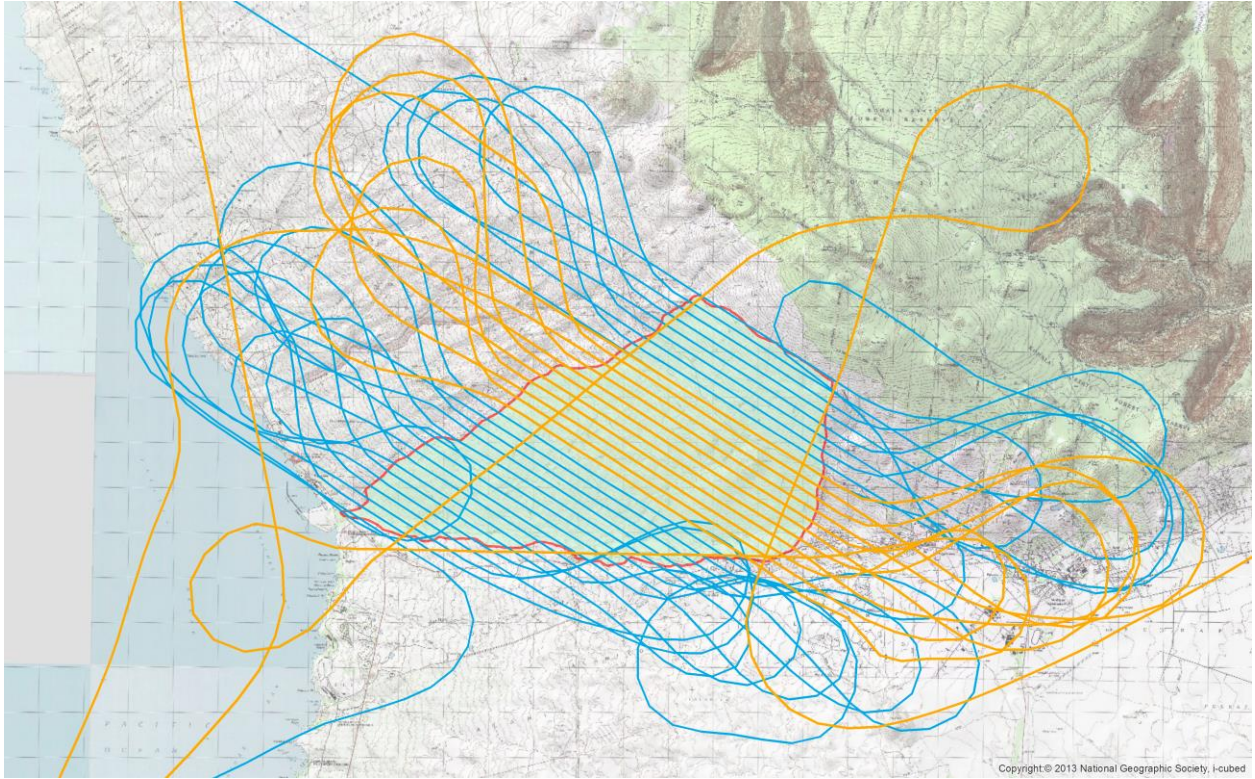


**Figure 2: Aircraft trajectories overlaid with the project boundary.**

## Tiling Scheme

The LiDAR data have been processed using a 1'500 x 1'500 meters tiling scheme anchored on the delivery tiles grid. The project AOI was slightly extended to include an additional study area being worked on by Kohala Center and UH-Hilo. This modified AOI was then buffered by 75 m. Only the data located inside this buffer and the AOI have been processed.

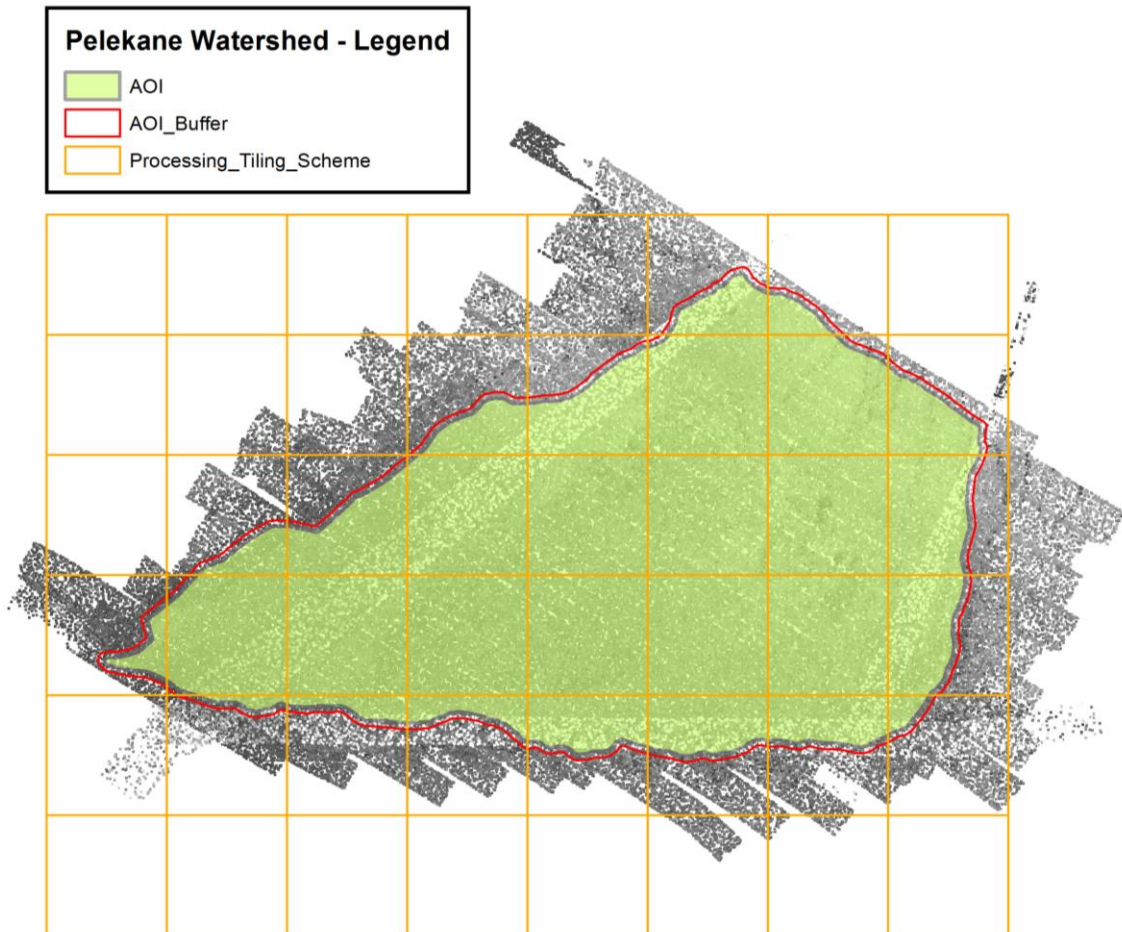


**Figure 3: Processing tiling scheme AOI and AOI-buffer overlaid with the LiDAR data (intensity view).**

The LiDAR data are delivered using a unique tiling scheme made of 12 tiles. The tiles measure 3'000 x 3'000 meters and are anchored on round coordinates (i.e. X=204'000, Y=2'223'000). The name of each tile is given by the coordinate of its upper left corner, divided by thousand (204\_2223 for the example used here above).

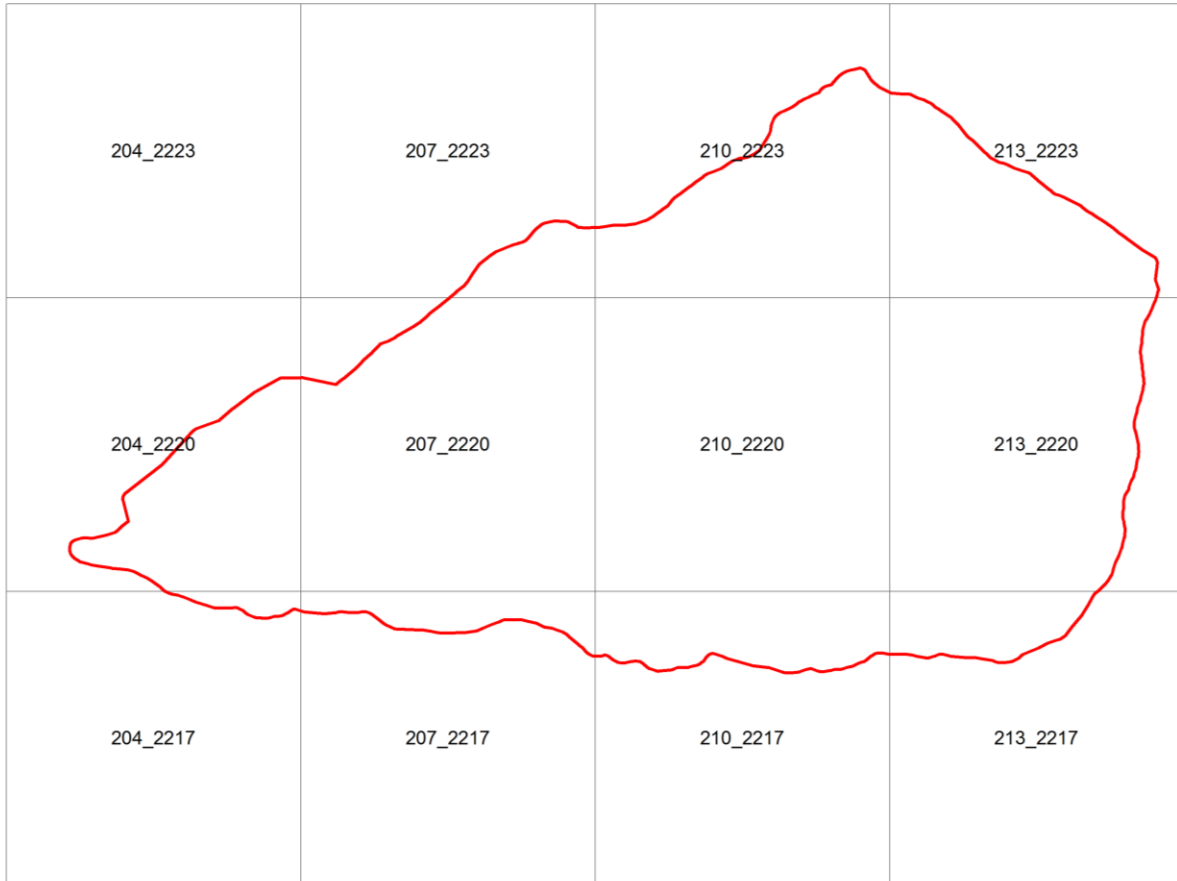


**Figure 4: Delivery tiling scheme and AOI-buffer for the Pelekane watershed.**

# LiDAR Quality Assessment

## *Data format*

The raw dataset is made of 38 flightlines saved in individual files. The Source ID is populated with respect with the flight order. The data are stored in LAS 1.4 PDRF 6. The intensity was normalized to 16 bit and the scan angles were limited during the acquisition. As result, the intensity values are ranging from 16 to 65520 and the scan angle fluctuate between -18 and +19 degrees (maximum FOV=38 degrees). All these information are summarized in the Figure 5.

## *Trajectory*

Since the LiDAR measurements are made from a plane which is flying several thousand feet above the ground, it is very important to monitor the trajectory of the aircraft with a high accuracy in order to get a high quality point cloud. A bad accuracy for the trajectory may lead to mismatch between overlapping flightlines or even local distortion of the point cloud. Both the relative and the absolute accuracy are therefore influenced by this critical parameter.

The Figure 6 and the Figure 7 present the evolution of the estimated accuracy of the plane's position for the two acquisition flights. The horizontal accuracy is slightly better than the vertical one, which is a normal situation for GPS measurements. Indeed, the geometry of the satellites constellation implies that the resection quality is better for the planimetry than for the altimetry. The trajectory appears to be accurate and will allow to get a reliable and uniform point cloud.

	File Name	File Source ID	LAS version	Point Format	System ID	Generation Software	Creation Day	Creation Year	Intensity Average	Intensity Min	Intensity Max	Scan Angle Min	Scan Angle Max	Scan Angle Standard Deviation
1	L1-1-237A-S1-C1_r.las	1	1.4	6	TUAV Orion	OptechLMS	252	2015	376.2738	16	10400	-17	17	10.8101
2	L3-1-237A-S1-C1_r.las	3	1.4	6	TUAV Orion	OptechLMS	252	2015	416.8769	16	6672	-17	17	10.7747
3	L4-1-237A-S1-C1_r.las	4	1.4	6	TUAV Orion	OptechLMS	252	2015	383.6793	16	9200	-17	17	10.7776
4	L5-1-237A-S1-C1_r.las	5	1.4	6	TUAV Orion	OptechLMS	252	2015	391.8985	16	7328	-17	16	10.7833
5	L6-1-237A-S1-C1_r.las	6	1.4	6	TUAV Orion	OptechLMS	252	2015	352.4082	16	13824	-17	16	10.735
6	L7-1-237A-S1-C1_r.las	7	1.4	6	TUAV Orion	OptechLMS	252	2015	352.9244	16	48160	-17	16	10.8076
7	L8-1-237A-S1-C1_r.las	8	1.4	6	TUAV Orion	OptechLMS	252	2015	323.6976	16	65520	-17	17	10.8074
8	L9-1-237A-S1-C1_r.las	9	1.4	6	TUAV Orion	OptechLMS	252	2015	306.91	16	65520	-17	17	10.8015
9	L11-1-237A-S1-C1_r.las	11	1.4	6	TUAV Orion	OptechLMS	252	2015	199.63	16	65520	-17	17	10.8094
10	L12-1-237A-S1-C1_r.las	12	1.4	6	TUAV Orion	OptechLMS	252	2015	198.4964	16	42032	-17	17	10.8081
11	L13-1-237A-S1-C1_r.las	13	1.4	6	TUAV Orion	OptechLMS	252	2015	200.5793	16	59792	-17	17	10.8102
12	L14-1-237A-S1-C1_r.las	14	1.4	6	TUAV Orion	OptechLMS	252	2015	189.8962	16	56112	-17	19	10.8029
13	L15-1-237A-S1-C1_r.las	15	1.4	6	TUAV Orion	OptechLMS	252	2015	191.8648	16	65520	-17	17	10.8092
14	L16-1-237A-S1-C1_r.las	16	1.4	6	TUAV Orion	OptechLMS	252	2015	181.8998	16	58512	-17	17	10.8092
15	L17-1-237A-S1-C1_r.las	17	1.4	6	TUAV Orion	OptechLMS	252	2015	192.1866	16	58224	-17	17	10.8107
16	L18-1-237A-S1-C1_r.las	18	1.4	6	TUAV Orion	OptechLMS	252	2015	177.6006	16	57840	-18	16	10.8096
17	L19-1-237A-S1-C1_r.las	19	1.4	6	TUAV Orion	OptechLMS	252	2015	178.6479	16	54368	-17	17	10.8093
18	L20-1-237A-S1-C1_r.las	20	1.4	6	TUAV Orion	OptechLMS	252	2015	169.0437	16	53040	-17	16	10.8108
19	L21-1-237A-S1-C1_r.las	21	1.4	6	TUAV Orion	OptechLMS	252	2015	174.3553	16	61152	-17	16	10.8106
20	L22-1-237A-S1-C1_r.las	22	1.4	6	TUAV Orion	OptechLMS	252	2015	165.9163	16	65520	-17	19	10.8145
21	L23-1-237A-S1-C1_r.las	23	1.4	6	TUAV Orion	OptechLMS	252	2015	172.4026	16	44832	-17	16	10.8098
22	L24-1-237A-S1-C1_r.las	24	1.4	6	TUAV Orion	OptechLMS	252	2015	147.7039	16	65520	-17	17	10.7897
23	L25-1-237A-S1-C1_r.las	25	1.4	6	TUAV Orion	OptechLMS	252	2015	133.484	16	65520	-17	16	10.8123
24	L26-1-237A-S1-C1_r.las	26	1.4	6	TUAV Orion	OptechLMS	252	2015	128.7172	16	65520	-17	16	10.5811
25	L27-1-238A-S1-C1_r.las	27	1.4	6	TUAV Orion	OptechLMS	252	2015	360.0739	16	65520	-17	17	10.7865
26	L28-1-238A-S1-C1_r.las	28	1.4	6	TUAV Orion	OptechLMS	252	2015	347.8885	16	58880	-17	17	10.8104
27	L29-1-238A-S1-C1_r.las	29	1.4	6	TUAV Orion	OptechLMS	252	2015	329.7098	16	34032	-17	17	10.7641
28	L30-1-238A-S1-C1_r.las	30	1.4	6	TUAV Orion	OptechLMS	252	2015	314.2215	16	65520	-17	16	10.8007
29	L31-1-238A-S1-C1_r.las	31	1.4	6	TUAV Orion	OptechLMS	252	2015	298.7415	16	7632	-17	16	10.811
30	L32-1-238A-S1-C1_r.las	32	1.4	6	TUAV Orion	OptechLMS	252	2015	291.662	16	65520	-17	17	10.8099
31	L33-1-238A-S1-C1_r.las	33	1.4	6	TUAV Orion	OptechLMS	252	2015	271.1952	16	65520	-17	17	10.7834
32	L34-1-238A-S1-C1_r.las	34	1.4	6	TUAV Orion	OptechLMS	252	2015	263.4753	16	65520	-17	17	10.8116
33	L35-1-238A-S1-C1_r.las	35	1.4	6	TUAV Orion	OptechLMS	252	2015	242.2696	16	22112	-17	17	10.8124
34	L36-1-238A-S1-C1_r.las	36	1.4	6	TUAV Orion	OptechLMS	252	2015	232.3483	16	21200	-17	17	10.8072
35	L37-1-238A-S1-C1_r.las	37	1.4	6	TUAV Orion	OptechLMS	252	2015	224.2266	16	65520	-17	17	10.7936
36	L38-1-238A-S1-C1_r.las	38	1.4	6	TUAV Orion	OptechLMS	252	2015	780.1465	16	65520	-17	16	10.8117
37	L39-1-238A-S1-C1_r.las	39	1.4	6	TUAV Orion	OptechLMS	252	2015	874.2052	16	65520	-17	17	10.7944
38	L40-1-238A-S1-C1_r.las	40	1.4	6	TUAV Orion	OptechLMS	252	2015	1181.8279	16	64448	-17	17	10.9239

Figure 5: Raw LiDAR files format and statistics.

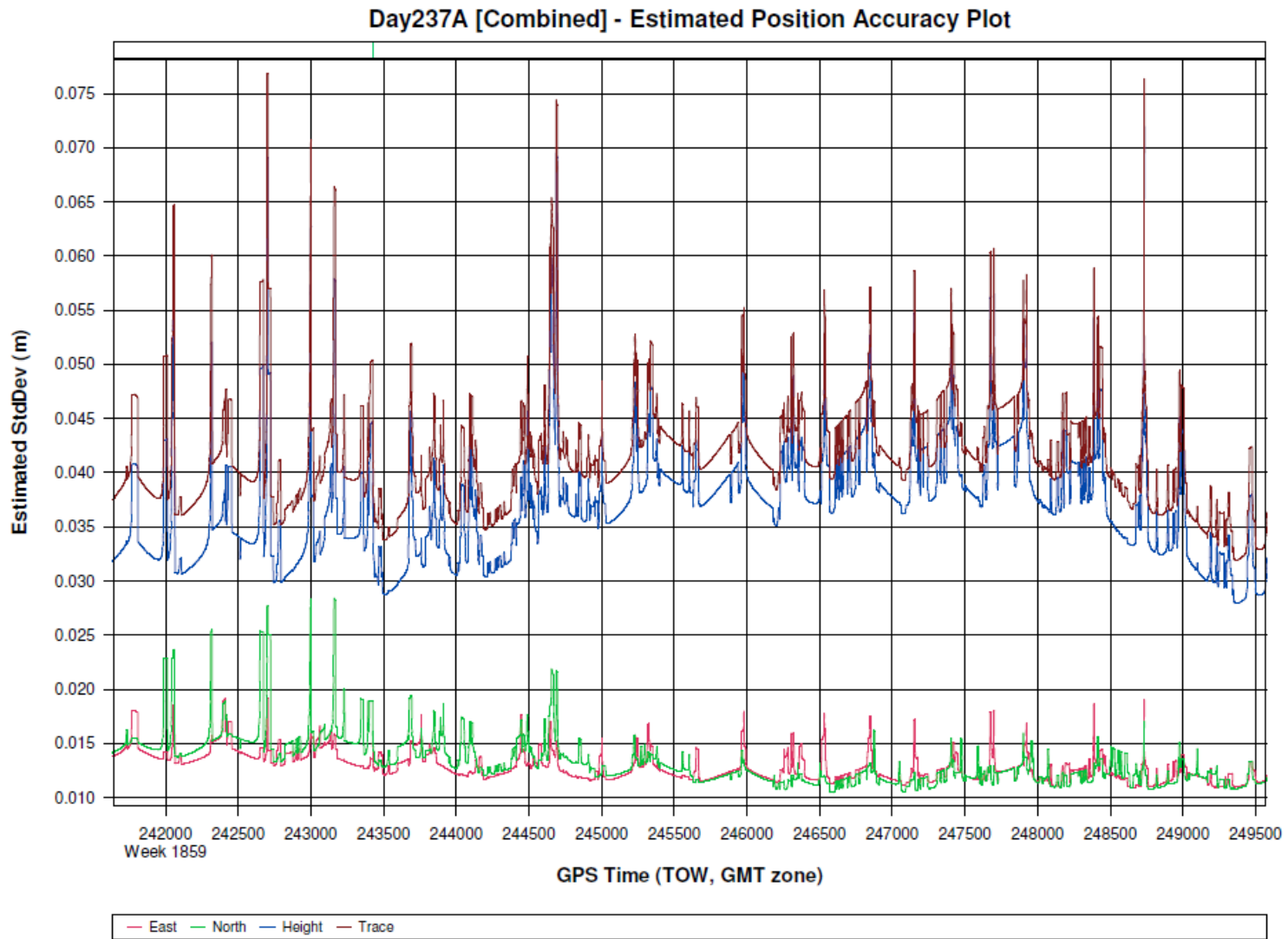


Figure 6: Trajectory accuracy for the August 25, 2015 acquisition.

Day238A [Combined] - Estimated Position Accuracy Plot

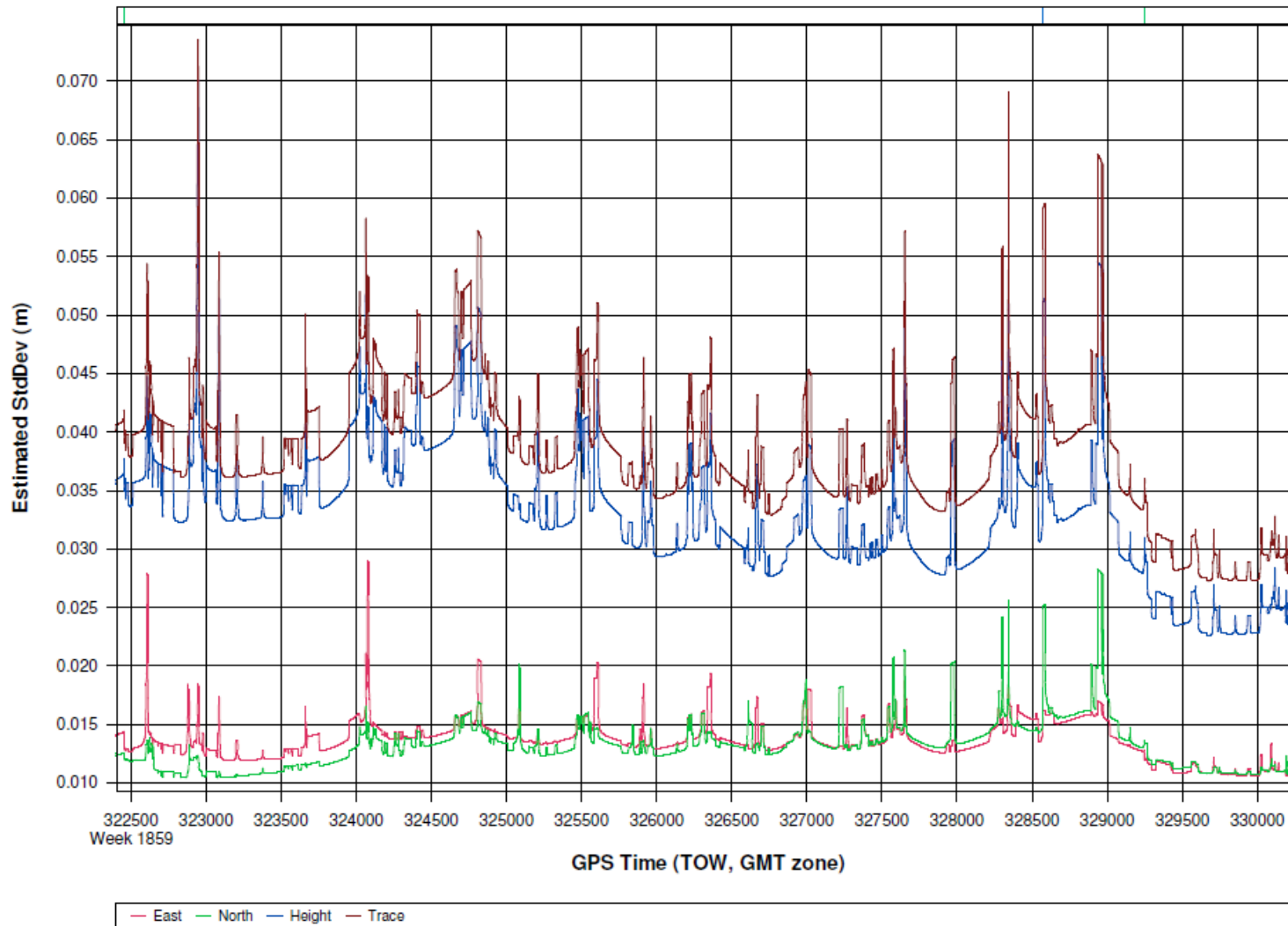


Figure 7: Trajectory accuracy for the August 26, 2015 acquisition.

## Coverage and swath-to-swath reproducibility

The swath-to-swath reproducibility is one of the first quality control checks that is performed on the LiDAR data, in order to have an idea of the relative accuracy of the point cloud. The internal point cloud accuracy is mainly affected by the quality of the trajectory, as well as by the LiDAR sensor calibration. After the flight, the LiDAR dataset is processed, and possible residuals of the sensor miscalibration are corrected in order to obtain a reliable point cloud.

To assess the quality of the swath-to-swath reproducibility, an image (Figure 8) of the differences between the single returns of overlapping flightlines was generated. This same image confirms that most of the area has been at least covered twice by the LiDAR beams. As displayed on the Figure 8, only the grey areas are single swath area. Most of them are located outside of the boundary of the project and should not be considered in the analysis.

In order to have a better understanding of the inter-swath quality of the dataset, two additional images are presented in the Figure 9. The two zoom images show that the different flightlines are matching well with each other. The red areas are generated by the vegetation, as the last echoes sometimes occur on a tree. However, the differences at the bare earth level are always presenting values lower than 0.08cm. This illustrates the good quality of the sensor calibration and of the GPS-IMU trajectory.

In order to better quantify the inter-swath accuracy, a set of 67 seamlines has been digitized in between the flightlines (Figure 10). Along each one of them, an algorithm extracted seeds points. For these places, the altimetry was extracted from the overlapping flightlines and compared. The generated dataset is then processed with a statistical approach in order to assess the quality of the relative accuracy of the point cloud. No less than 8229 seed points were defined for this project using the seamlines. The distribution of the vertical differences population is presented in the Figure 11. Other statistical indexes are summarized in the table below the Figure 11.

Based on all these results, we can affirm that the relative accuracy level of the Pelekane watershed LiDAR dataset meets the requirements of 8 cm as RMSEz and +/- 16 cm as maximum departure.

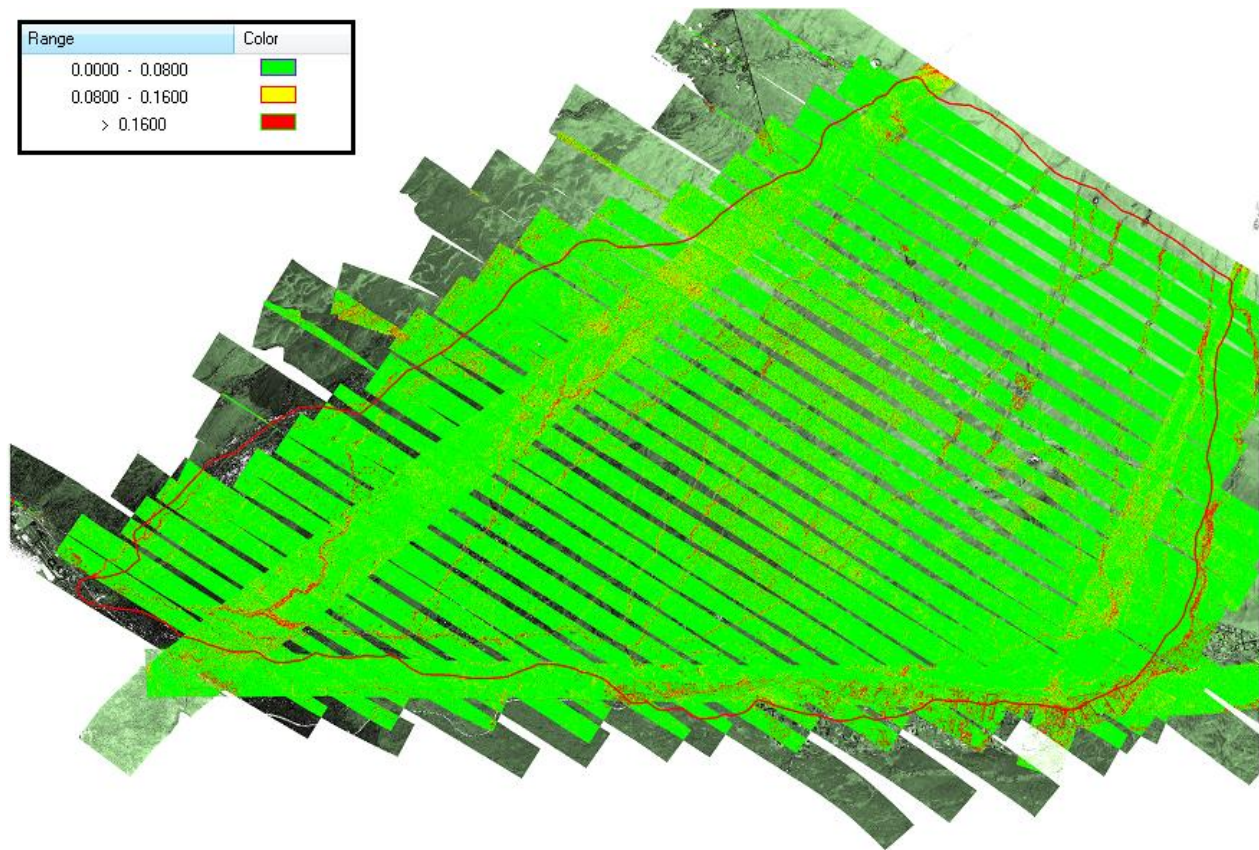


Figure 8: Swath overlap differences in meters for a 1m-cell grid, using single returns only.

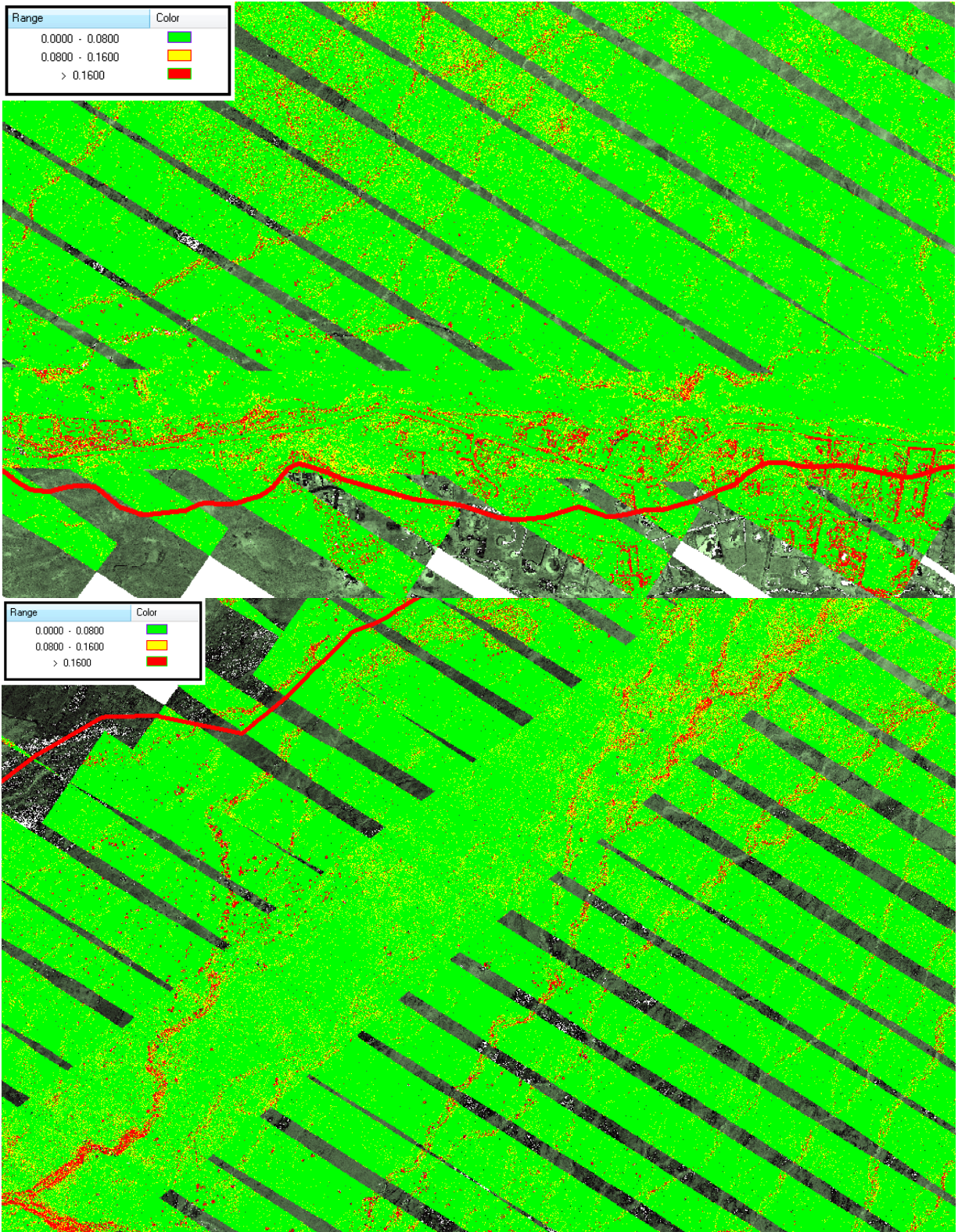
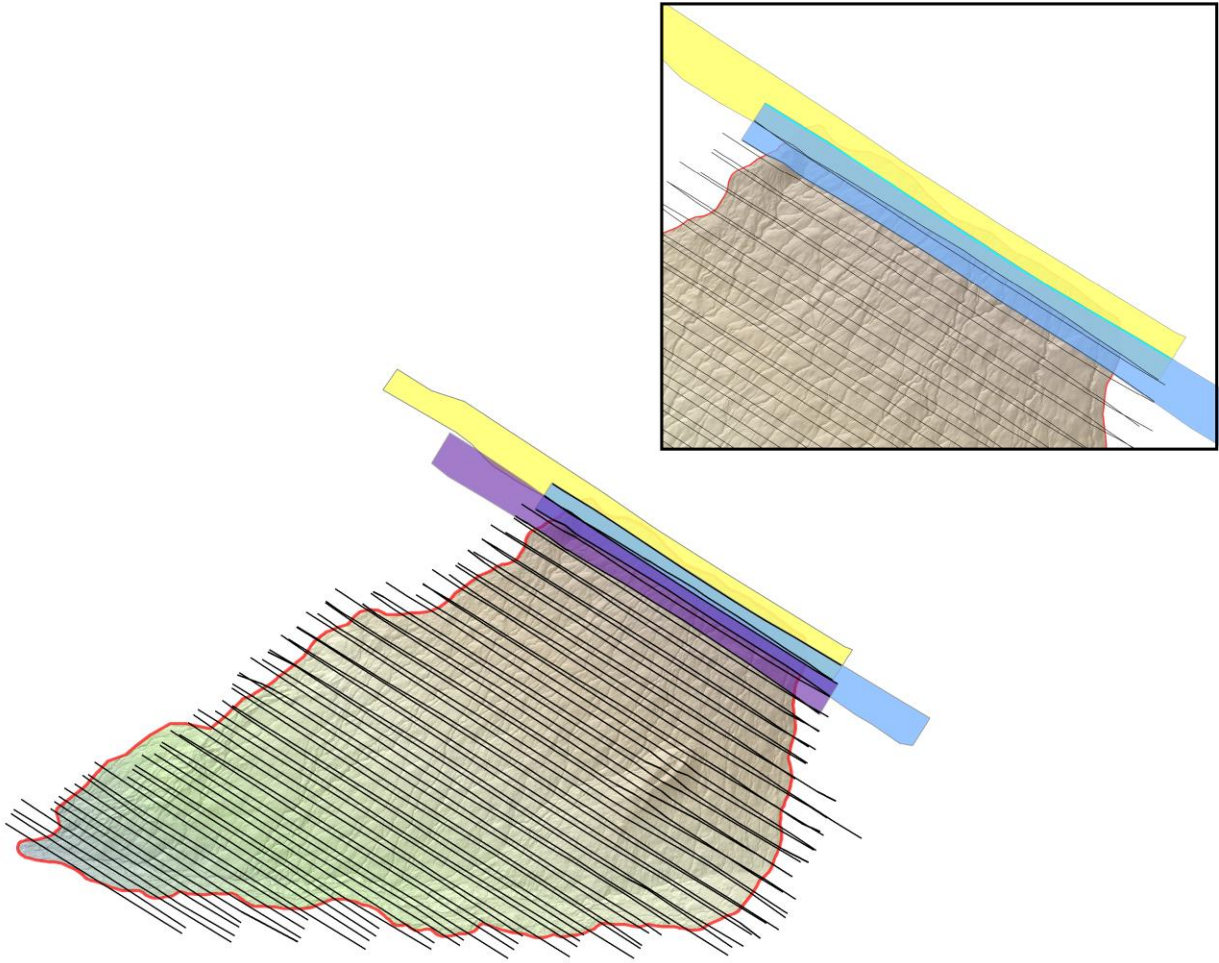


Figure 9: Two zooms over the swath-to-swath image (in meters).



**Figure 10: Seamlines between overlapping flightlines.**

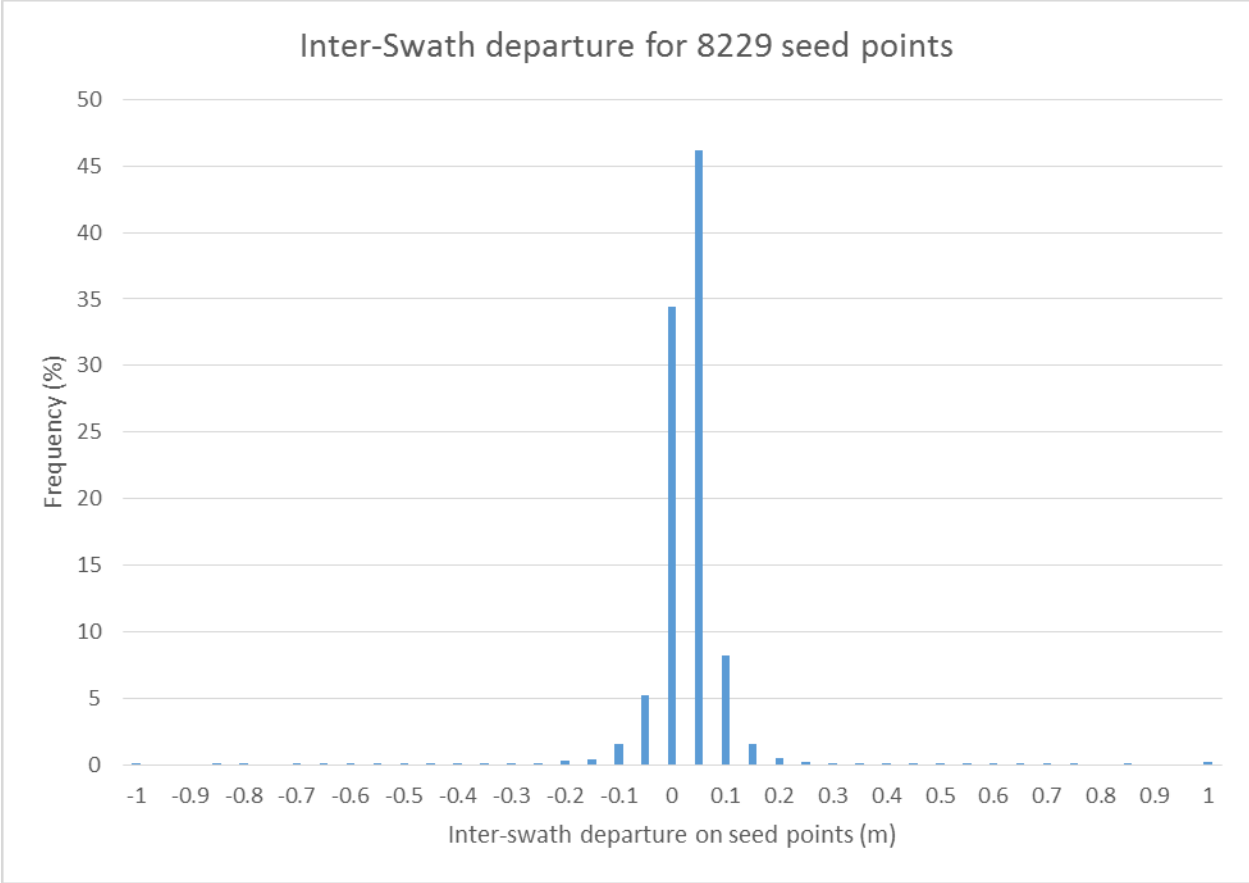


Figure 11: Distribution of inter-swath departure for 8229 seed points.

Inter-swath departures statistics	
Minimum departure	-86.9 cm
Maximum departure	84.6 cm
Average departure	0.5 cm
Median departure	0.5 cm
Standard deviation	6.5 cm
Root Mean Square Error, vertical	6.5 cm
Vertical Accuracy @ 95%	12.8 cm

## Absolute accuracy

In order to assess the absolute accuracy of the LiDAR data, a set of 37 Ground Control Points (GCP) have been surveyed. These points are well distributed over the project area. The following table presents the coordinates of each GCP together with the corresponding soil cover category. The projection used is UTM Zone 5N with GRS80 as vertical datum and NAD83 PA11 as horizontal datum. Units are in meters.

### LiDAR for Pelekane Watershed

#### List of the 37 Ground Control Points

NAD83 PA 11 GRS 80 UTM 5N , Units: Meter

NAME	Easting	Northing	Elevation	Soil Cover	NAME	Easting	Northing	Elevation	Soil Cover
P101	212263.890	2220771.793	1050.724	VVA	P305	213405.768	2219290.606	990.643	NVA
P102	211410.527	2220127.789	888.082	NVA	P306	215070.964	2218492.292	933.887	NVA
P103	210697.076	2219401.731	745.272	VVA	P307	214628.126	2216569.615	642.689	NVA
P104	210361.336	2219105.944	687.460	VVA	P308	213001.829	2216495.407	572.317	NVA
P105	209616.615	2218267.430	529.602	NVA	P309	211527.733	2216572.833	495.676	NVA
P106	209439.027	2218039.935	489.822	NVA	P310	213085.324	2218392.943	825.180	NVA
P107	208840.366	2217677.636	394.994	NVA	P311	214490.609	2220457.155	1249.720	VVA
P108	205212.924	2217533.455	67.823	NVA	P312	212568.650	2221033.773	1118.987	VVA
P109	207252.568	2217526.883	255.560	VVA	P313	212931.210	2221500.874	1222.319	VVA
P110	207603.023	2218133.704	363.592	VVA	P314	213464.613	2221663.828	1305.878	VVA
P111	206648.449	2218777.900	336.192	NVA	P401	211940.027	2220494.621	979.592	VVA
P112	206637.963	2218776.968	335.409	NVA	P402	211038.956	2219689.665	807.678	NVA
P113	206731.525	2218861.817	349.133	NVA	P403	211082.932	2219246.886	760.904	NVA
P114	206448.882	2218740.258	304.406	NVA	P404	209986.598	2218732.148	614.409	NVA
P115	206233.341	2218562.177	261.878	NVA	P405	209986.598	2218732.148	614.406	NVA
P301	208816.659	2216379.552	321.457	NVA	P406	209545.446	2218017.116	498.447	VVA
P302	209278.782	2216399.564	349.526	NVA	P407	208954.882	2217323.412	371.348	NVA
P303	212425.858	2220881.021	1073.615	NVA	P408	205129.517	2217368.668	55.782	VVA
P304	212692.814	2220181.979	1039.136	NVA					

The spatial distribution of the ground control points is depicted on the Figure 12.

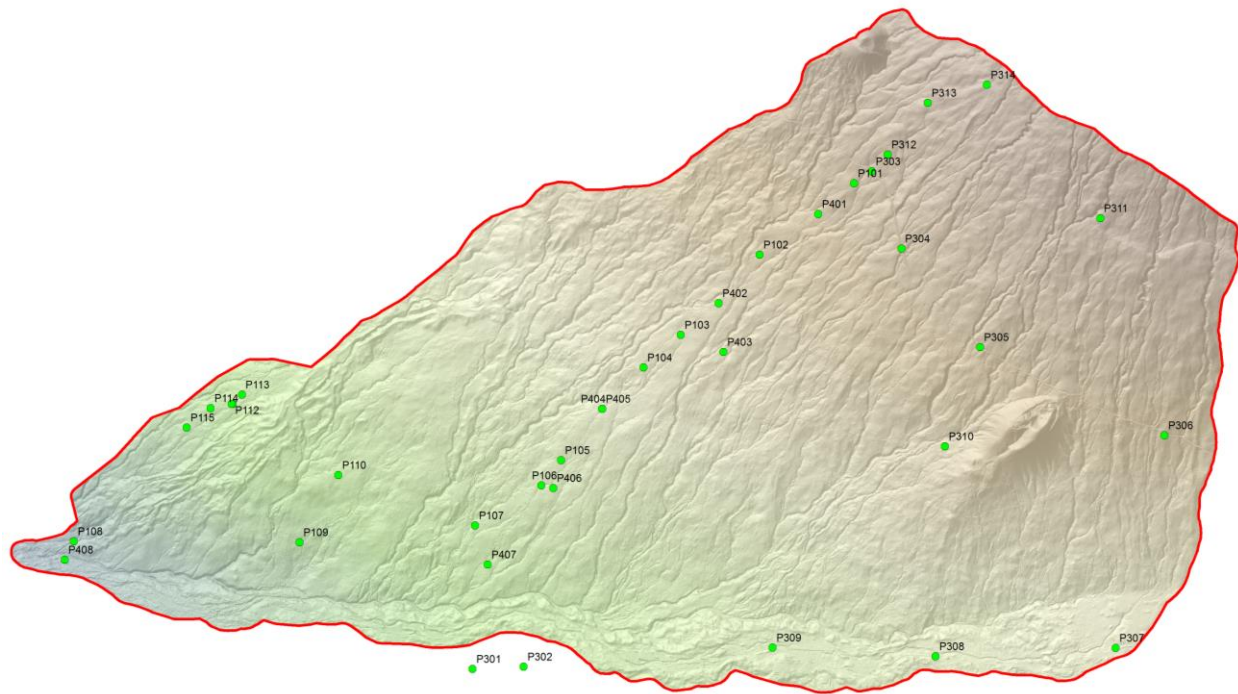


**Figure 12: Spatial distribution of the 37 GCP over the project area.**

The absolute accuracy of the LiDAR dataset was assessed by comparison with the GCP. After a first comparison with the LiDAR point cloud, it appears clearly the point cloud is affected by a global trend.

**The residuals distribution presented in the**

Figure 13 highlights the skew. The fact that the median (robust estimator) is bigger than the average also indicates that the dataset is affected by an absolute shift.

### Global analysis

The following figures represent the distribution of the vertical residuals computed on the 35 GCP that are located within the project's AOI. The points P301 and P302 are outside of the study perimeter and therefore they are not in use for this analysis.

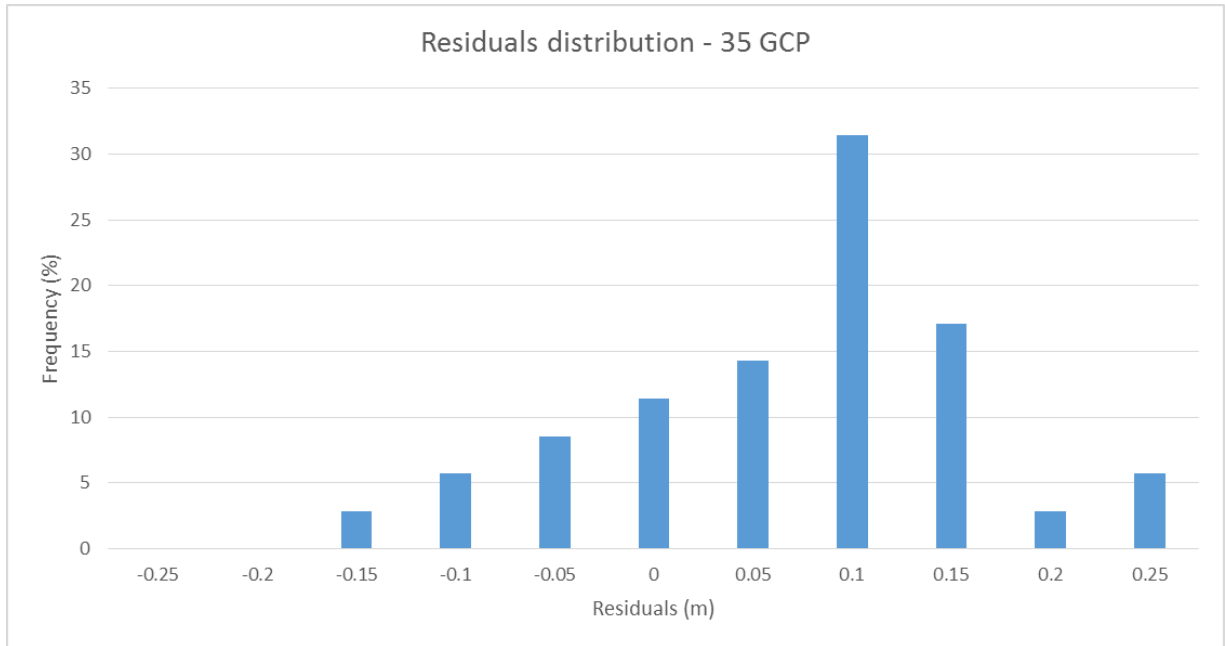


Figure 13: Residuals distribution computed on 35 GCP.

Several additional statistical indexes have been computed and are listed in the table below.

Statistics computed for the residuals	
Minimum residual	-17.3 cm
Maximum residual	24.4 cm
Average residual	4.4 cm
Median residual	6.3 cm
Standard deviation	8.9 cm
Root Mean Square Error, vertical	9.9 cm
Vertical Accuracy @ 95%	19.3 cm

Based on these results, a global shift was applied to the LiDAR point cloud, in order to improve the absolute accuracy of the dataset. The applied shift has a magnitude of -4.4 cm, and corresponds to the inverse value of the average computed on the 35 GCP.

The following illustration shows the distribution of the residuals computed on the shifted point cloud with the 35 GCP. Again, the final detailed statistics are presented in a table below.

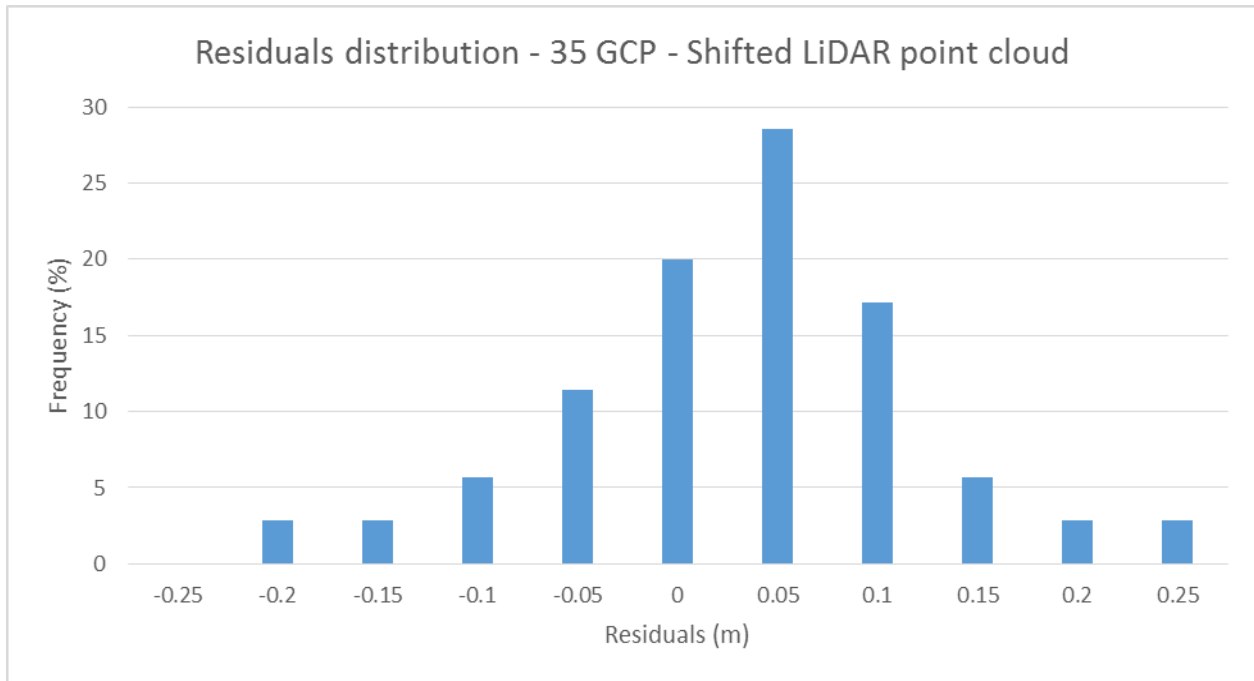


**Figure 14: Distribution of the residuals computed with 35 GCP after the LiDAR global shift.**

<b>Statistics computed for the residuals of the shifted LiDAR</b>	
<b>Minimum residual</b>	-21.3 cm
<b>Maximum residual</b>	20.4 cm
<b>Average residual</b>	0.4 cm
<b>Median residual</b>	2.3 cm
<b>Standard deviation</b>	8.9 cm
<b>Root Mean Square Error, vertical</b>	8.8 cm
<b>Vertical Accuracy @ 95%</b>	17.3.cm

These last results show that the global vertical accuracy at 95% of the LiDAR point cloud with a value of 17.3cm is within the requirements of the project (19.6 cm).

The following figure presents the residuals values on a map. It appears that no spatial pattern in the vertical differences between the GCP and the LIDAR can be observed.

### GCP residuals (m)

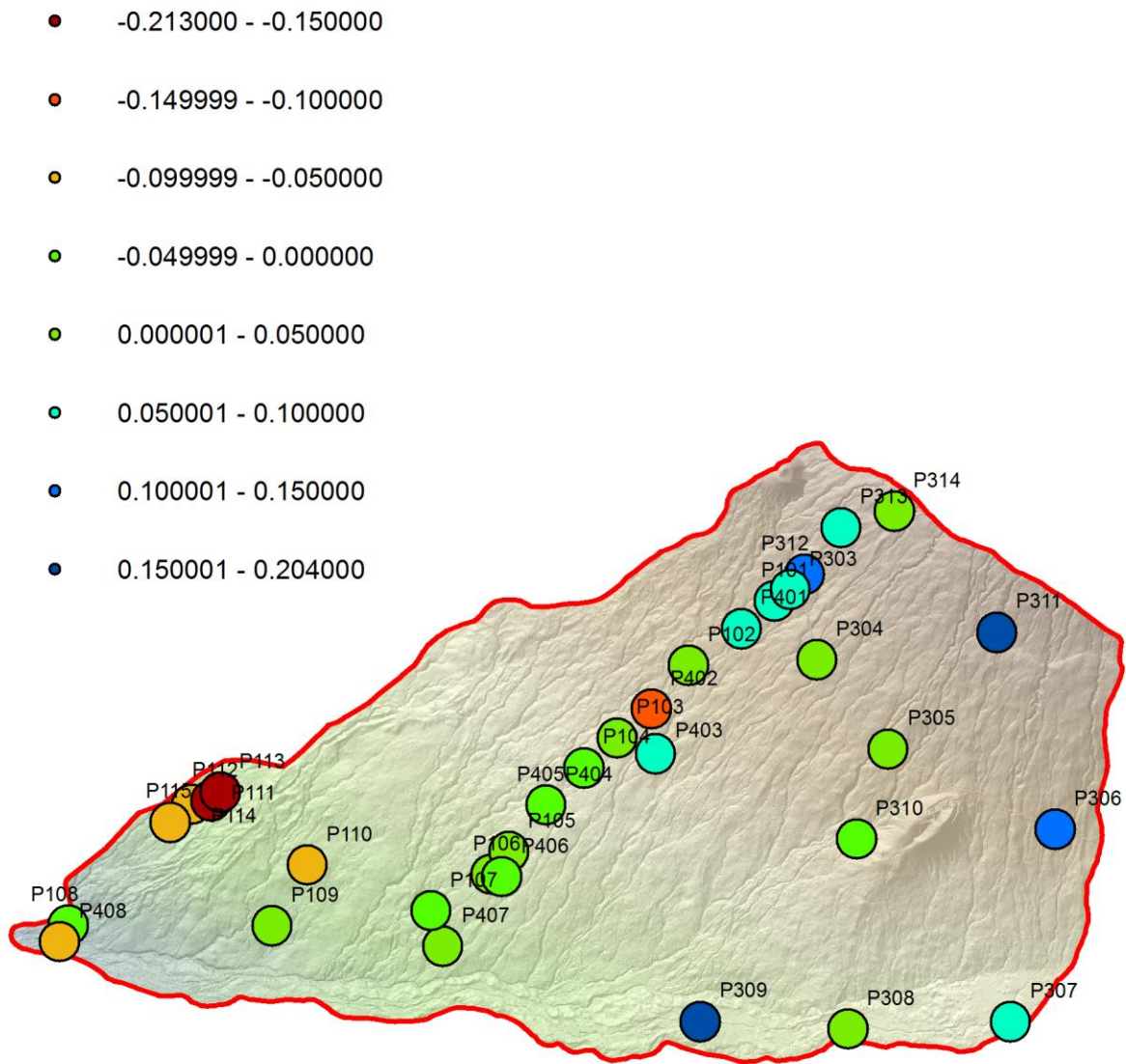
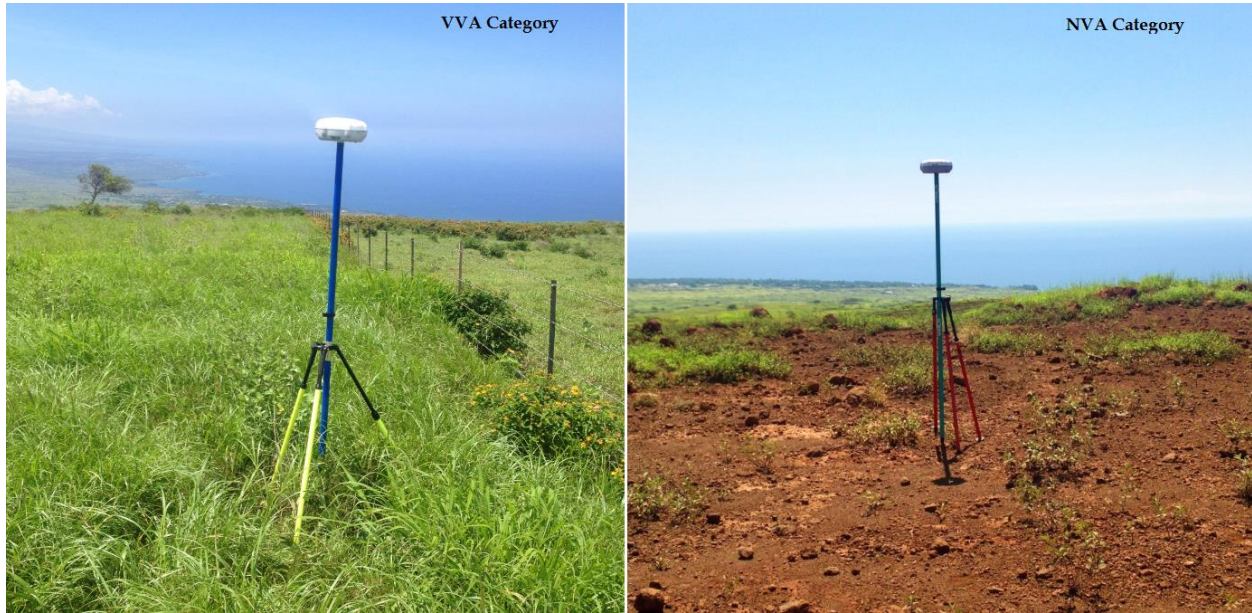


Figure 15: Residuals values overlaid with a map of the project area.

## Analysis by soil cover category

In order to better sense the quality of the data and to conform to the USGS specifications, the GCP were classified into two soil cover categories. The comparison between the LiDAR dataset and the control points was therefore conducted again, in order to quantify the Nonvegetated Vertical Accuracy (NVA) and the Vegetated Vertical Accuracy (VVA) The Figure 16 presents an example of each of the above soil cover classes.



**Figure 16: Comparison between VVA and NVA Ground Control Points.**

The tables below summarize the results of this accuracy check with respect to these two categories. The NVA results are really affected by two extreme values (min and max). If these points are considerate as outliers (probably bad GPS measurements), the final accuracy for the NVA drops below the VVA numbers.

### Absolute vertical accuracy analysis by soil cover category

Values in meter

VVA	Min. value	-0.092
	Average	0.030
	Median	0.041
	Max. value	0.170
	Std Dev	0.077
	RMSEz	0.080
	95 % acc z	0.156

NVA	Min. value	-0.213
	Average	-0.009
	Median	0.018
	Max. value	0.204
	Std Dev	0.094
	RMSEz	0.092
	95 % acc z	0.181

NVA robust	Min. value	-0.159
	Average	-0.010
	Median	0.018
	Max. value	0.113
	Std Dev	0.073
	RMSEz	0.072
	95 % acc z	0.142

## Point Density

The point density computed using the first returns only for each tile shows that the most of the project area is covered at least with the design pulse density of 8 points per square meter (ppsm) corresponding to a point spacing distance 0.33 meter. The tiles located on the edge of the project exhibit usually skewed values due to boundary effect.

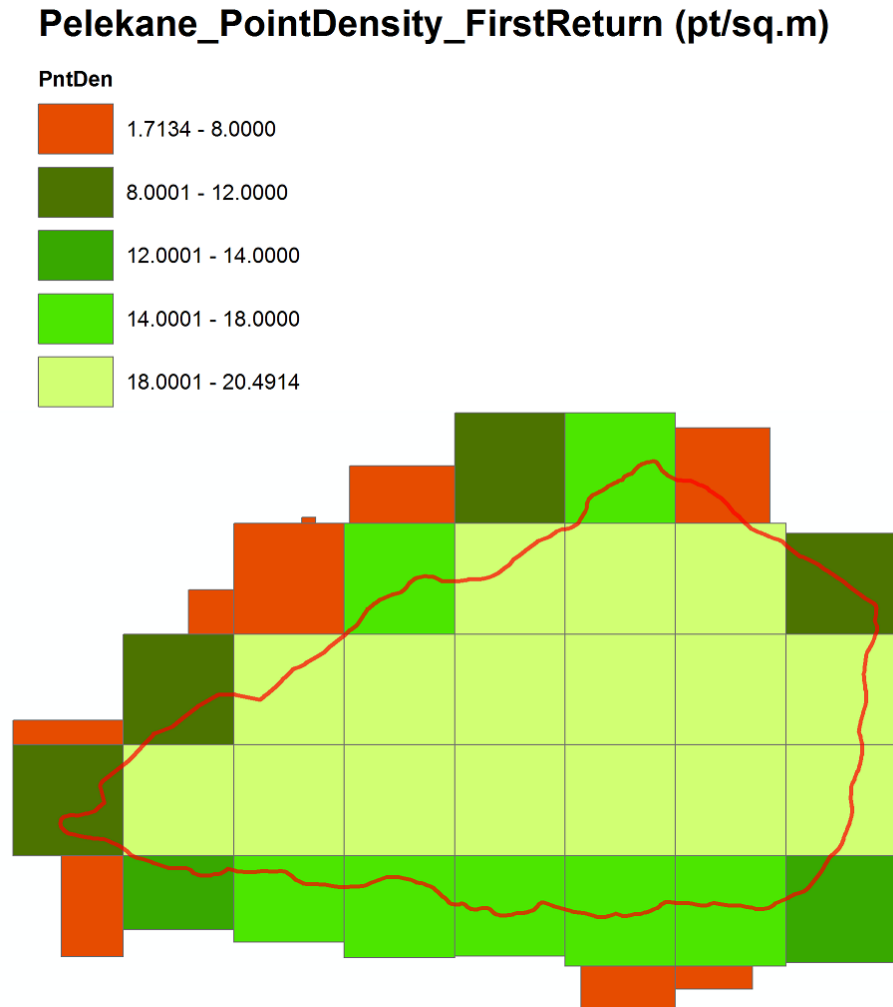


**Figure 17: First return point density computed for each LiDAR tile.**

In order to get a better understanding of the point density and of their spatial distribution a more extensive study has been done. The first step consists in computing the Aggregate Nominal Pulse Density (ANPD) for an area of 1 square kilometer that is representative of the entire project. This test area is displayed on the Figure 18.

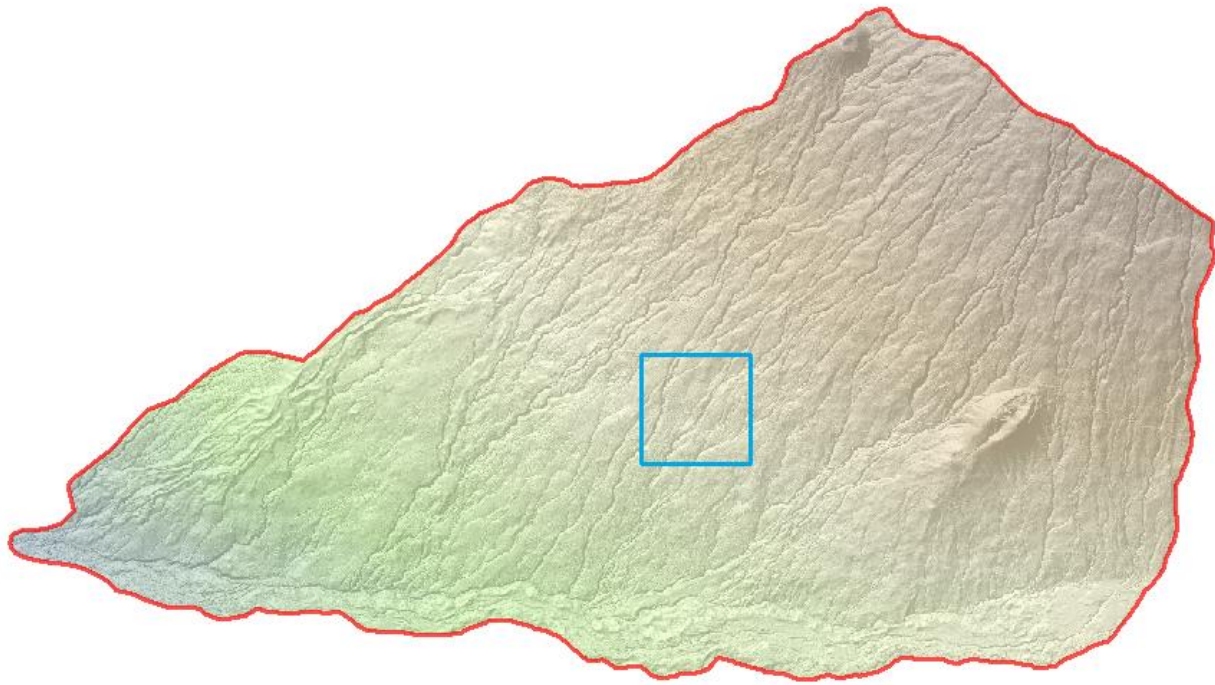


**Figure 18: Representative area (1 sq. km) for point density and spatial distribution assessment.**

The ANPD is obtained by dividing the number of point included in the test area by its surface.

$$ANPD = \frac{Point\ s\ number}{Surface}$$

The USGS requires the user to compute the ANPD only on the geometrically usable center part of the swaths (typically 95 percent), and only on the first-return echoes. As presented previously in the report, the maximum scan angle is 19°. Therefore, the scan angle has been limited to 18° for the purpose of this assessment, restraining the study on the central part of the swaths as specified in the USGS specifications.

The ANPD for this project is equal to 19.8 points per square meter.

The study of the point density and of the spatial distribution should be based on a grid with a cell size equivalent to 2 times the Aggregate Nominal Point Spacing (ANPS). The ANPS is obtained by analyzing the same square kilometer test area.

For this project, the ANPS is computed with the following formula:

$$ANPS = \sqrt{\frac{Surface}{Number\ of\ points}} = \sqrt{0.0502957} = 0.225\ meter$$

A density grid with a cell size equivalent to twice the ANPS is then generated, using the first-return echoes that have a scan angle between  $-18^\circ$  and  $+18^\circ$  as input dataset. For gridding purposes, the cell size was rounded to 0.5 meter instead of the 0.45 meter given by the strict formula. In order to ensure a point density of one point per cell, the required density is equal to the inverse of the cell size. The density threshold was therefore set to 2. This computation leads to the grid presented in Figure 19.

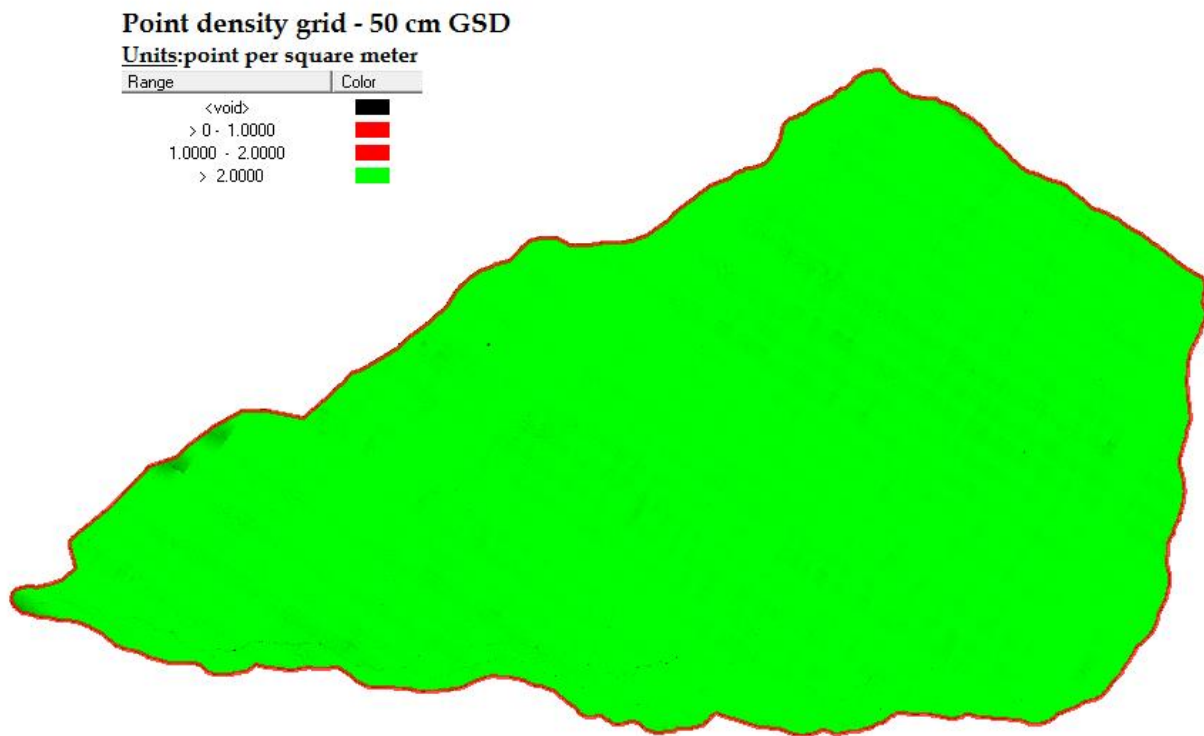


**Figure 19: Point density grid, 50 cm cell size.**

In order to quantify the percentage of cells that contain at least one point, the grid data were summarized with a frequency study. This last analysis was conducted within the square kilometer perimeter previously described. The results are presented in table below.

	<b>Cell Count</b>	<b>Percentage</b>
<b>Cell with at least one point</b>	3984623	99.57
<b>Cell with less than one point</b>	17377	0.43
<b>TOTAL</b>	4002000	100

Given all these results, we conclude that the point density as well as the associated spatial distribution meet the USGS LiDAR specifications.

## Final product overview

For this project area, a Digital Terrain Model with a resolution of 1m is delivered together with the LiDAR point cloud. The model is free of voids, tile-boundary effect or project boundary artifacts. The Figure 20 offers an overview of the DTM grid overlaid with the derived hillshade model and the AOIs.

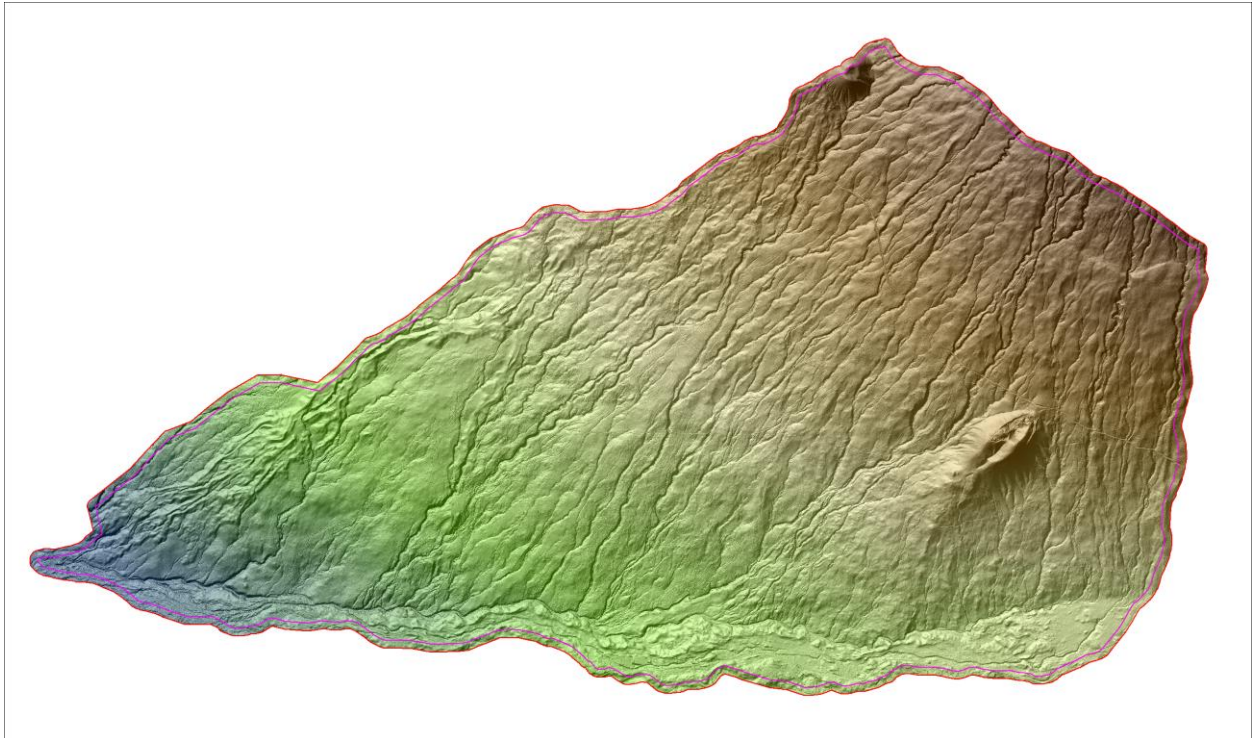


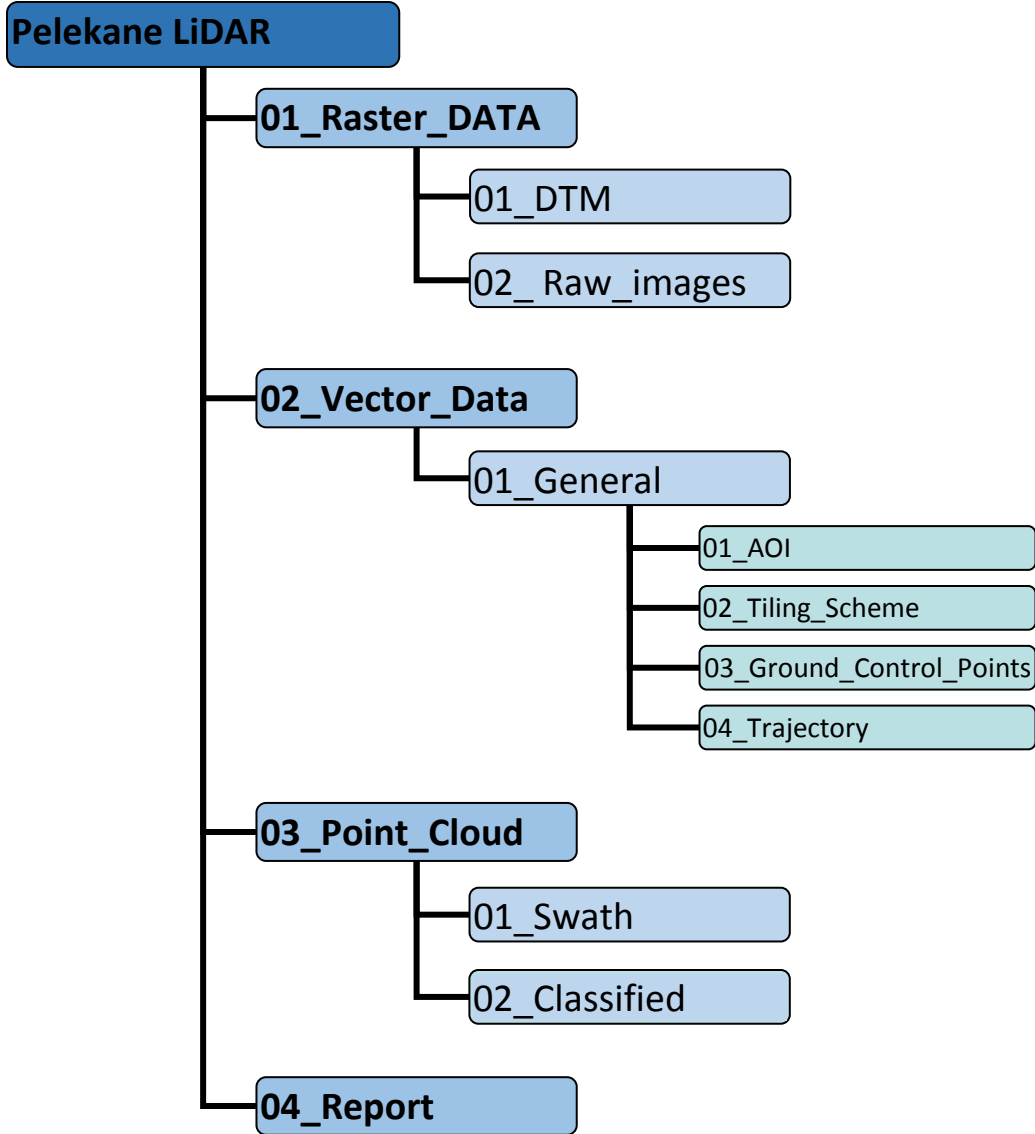
**Figure 20: Digital Elevation Model – 1 meter grid combined with the corresponding hillshade and the AOIs.**

## Projection/Datum and Units

<b>Projection</b>		UTM Zone 5 North
<b>Datum</b>	<b>Vertical</b>	Geodetic Reference System 1980
	<b>Horizontal</b>	NAD83 PA11
<b>Units</b>		Meters

## Deliverables

All of the deliverables are saved on two USB 3.0 hard drive. The architecture used to organize the delivery folder is presented on the next page.





Tetra Tech Geomatic Technologies Group

3746 Mount Diablo Blvd Suite 300

Lafayette, CA 94549

